American Journal of Sciences and Engineering Research

E-ISSN -2348 – 703X, Volume 6, Issue 6, 2023

Impact study of a Vertical Axis Tidal Turbines Column's Torques on the Electromechanical Outputs of a Permanent Magnet Synchronous Generator

Télesphore RANDRIAMAITSO[1]*, Solo Njara RHEVIHAJA[2], F. Philibert ANDRINIRINIAIMALAZA[1], Chrysostome ANDRIANANTENAINA[1], Théodore TOTOZAFINY [3]

[1]*University of Mahajanga, Higher Institute of Sciences and Technologies, Building Ex-LOLO Majunga-be, Mahajanga, Madagascar*
[2]*University of Mahajanga, Life Engineering and Modeling Doctoral School (EDGVM), Mahajanga, Madagascar*
[3]*University of Mahajanga, Faculty of Sciences, Technologies and Environment, Mahajanga, Madagascar*

ABSTRACT: *The objective of this article is to observe the effect of the torque provided by a column of turbines offset or not with vertical axis of a tidal turbine on its electromechanical output quantities such as the rotation speed, the currents and the voltages of the PMSG when the tidal turbine is equipped or not with the regulation system. In this study, this torque is determined by the DMST method. And, the PMSG Park model is used. In addition, the chosen control system includes a PWM rectifier, PI correctors and an optimal TSR MPPT control. The latter considers the fixed reference rotation speed at each flow speed. Three turbines mounted in a column with the same radius of 455mm and height of 824mm were considered. The simulation was carried out with operation at maximum average efficiency of the column of three turbines and a flow of 1.5 m/s. Without a control system, the tidal turbine output quantities with a column of non-offset turbines have more undulating amplitudes compared to if they are offset. These output quantities are improved in the presence of regulation. They can be further improved by seeking the reference rotation speed as a variable in order to minimize the error between the measured rotation speed and the reference speed.*

Keywords: *Tidal turbines column, vertical axis, PMSG, DMST, control, electromechanical output.*

I. INTRODUCTION

Currently, the energy we use daily comes essentially from usual sources such as fossil fuels (oil, gas, coal) [1] [2]. Their major disadvantage lies in the very rapid exhaustion and the emission of gases which enormously pollute the atmosphere. Faced with the constraints posed by fossil fuels, the best possible solution would be to use renewable energies which have the advantage of being abundant and inexhaustible in the millennia to come. It is in this situation that tidal energy presents itself today as one of the most interesting sources of renewable energy, thanks to its enormous global potential estimated at a power of 100 GW [3], which represents a considerable deposit.

Tidal turbines are turbines that recover kinetic energy from river or sea currents. They are somehow equivalent to wind turbines. To produce energy, tidal turbines will need a current speed greater than 1m/s on average [4].

The Permanent Magnet Synchronous Generator (PMSG) is widely used in tidal turbine applications, in particular, because of its good conversion efficiency (close to 99% compared to the asynchronous machine) [3]. The synchronous machine allows operation as well at low speed (system direct drive) than at high speed (indirect

 Received-12-12-2023, Accepted- 21-12-2023

drive system), so it can be coupled or not with a speed multiplier [5]. Two main categories of tidal turbines exist: those with a horizontal axis of rotation and those with a vertical axis of rotation. This study considers a tidal turbine with a column of turbines with a vertical axis of rotation equipped with a direct-drive permanent magnet synchronous generator (PMSG). The PMSG transforms mechanical energy into electrical energy.

The turbines on a column can be offset relative to each other. Studies show that the vertical turbine provides pulsating torque [6], [7], [8], [9]. So, our objective is to observe by simulation, the impact of the oscillation of the torques of the column of turbines offset or not with vertical axis on the electromechanical output quantities of the tidal turbine, namely the rotation speed, the currents and the tensions of the PMSG. The simulation requires modeling the tidal system without or with a control system. The latter uses the MPPT tip speed ratio (TSR) method. or (MPPT with optimal TSR) [10] with PI corrector [11], [12] to control the turbine and the vector control of the PMSG associated with PI corrector and MLI rectifier based on bipolar transistor (IGBT) [13], [14], [15] . Then, the turbine torque is determined by DMST method [16], [17], [18], [19]. Finally, the PMSG PARK model [20], [21] is used.

II. MATERIAL AND METHODS

2.1. Presentation of the studied system

The tidal turbine considered comprises three- phase PMSG and a vertical axis tidal turbine column of which has three straight blades with height H, radius R, profile NACA0018 [22], and chord length C according to *Figure 1* . The turbine column is placed in a velocity flow $\vec{U}_\infty$ assumed to be constant and uniform and rotates with a rotational speed ω fixed by the electric generator. This last provides currents and voltages characterized by a frequency and amplitudes. It supplies an R-L load.

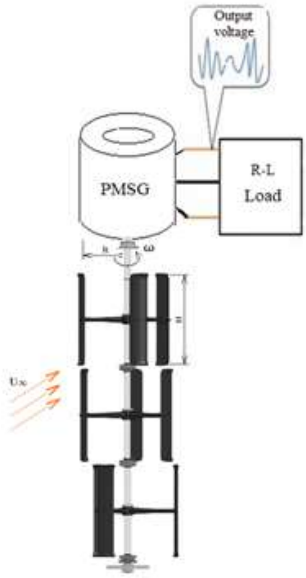

Figure 1: Presentation of the tidal turbine with three turbine columns

2.2. Turbine modeling

2.2.1. Power coefficient and tip speed ratio

The mechanical power P_m that can be produced by a tidal turbine represents a fraction C_P of fluid's hydrodynamic power, in formula (1).

$$P_m = \frac{1}{2} C_P \rho A U_\infty^3 \quad (1)$$

Where C_P is the power coefficient characterizing the hydrodynamic performance of a tidal turbine, ρ the density of water (kg/m^3), A the surface swept by the blades (m^2), and U_∞ the tidal speed (m/s). The coefficient of power C_P does not exceed the limit of 59% which constitutes the Betz limit [18] .

Figure 2 presents the evolution of the power coefficient according to the tip speed ratio λ which is expressed by equation (2).

$$\lambda = \frac{\omega R}{U_\infty} \tag{2}$$

The optimum value of the tip speed ratio (λ_{opt}) corresponding to the maximum power coefficient is a characteristic of the turbine. To control a turbine, the reference speed for optimal MPPT TSR control method is given by formula (3) [15].

$$\omega_{réf} = \frac{\lambda_{opt} U_\infty}{R} \tag{3}$$

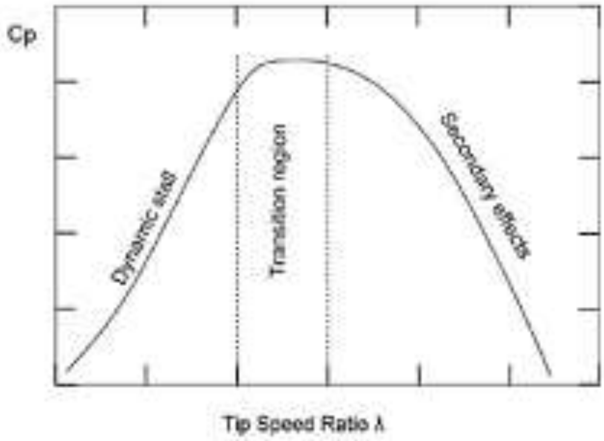

Figure 2: Evolution of the power coefficient as a function of the advance parameter [7]

2.2.2. Forces and speeds

The blade placed in a flow is subjected to two forces (*Figure 3):* the drag force parallel to the direction of the flow, denoted D, and the lift force perpendicular to the flow and denoted L.

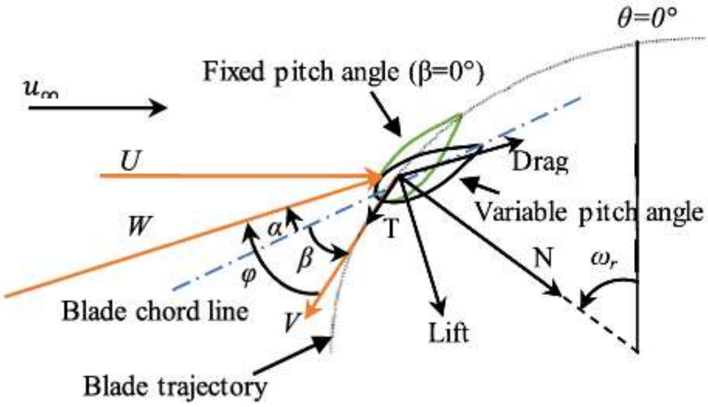

Figure 3: Forces and velocities acting on the blade of a turbine [23]

Angles α, β, and θ are respectively angle of attack or angle of incidence, a pitch angle, and the azimuth angle. The available torque on a tidal turbine is given by the force $\vec{F}_T$, tangential to the circle of rotation.

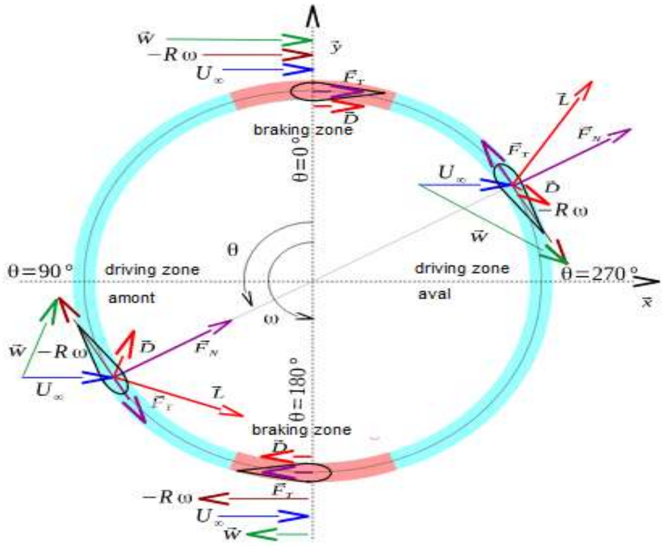

Figure 4: Analysis of driving and braking zones in a vertical axis turbine [18]

On the other hand, the force $\vec{F}_N$ is a decisive force for the mechanical resistance of the blades because it is very variable and generates an alternating loading on the blade. The rotor surface can be divided into four zones: two driving zones and two braking zones.

The surface of the rotor can be broken down into four zones: two motor zones and two braking.

These two driving zones are located in part of the upstream half-disc and part of the downstream half-disc of the turbine according to *Figure 5.*

2.2.3. Determining the torque, power and efficiency of a vertical axis tidal turbine using the DMST model

Figure *5* represents the tidal turbine modeled by two upstream and downstream actuator discs. There is an equilibrium position located between the upstream zone and the downstream zone whose speed of passage in this zone is called equilibrium speed U_e. When the fluid passes through this zone, the pressure is equal to that of the undistributed flow upstream of the turbine.

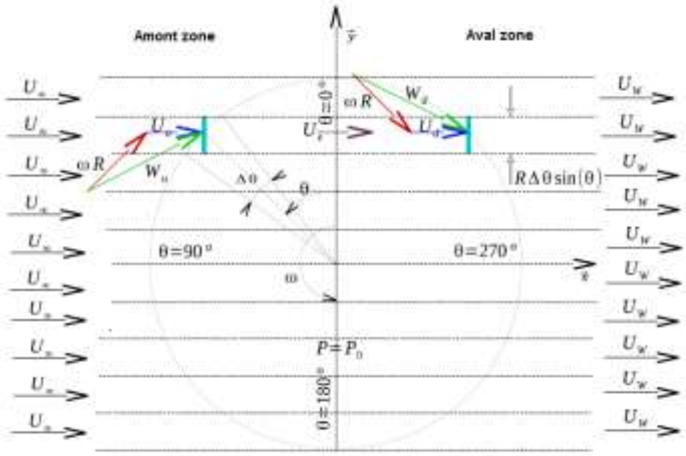

Figure 5: Model with multiple current tubes and two actuators (seen from above) [18]

The induction factors a_u and a_d respectively of the upstream and downstream half-disk are defined by relations (4) and (5).

$$a_u = \frac{U_\infty - U_u}{U_\infty} \tag{4}$$

$$a_d = \frac{U_e - U_d}{U_\infty} \tag{5}$$

The DMST model using the laws of fluid mechanics with the actuator disk theory allows to establish non-linear equations relating the induction factors, the hydrodynamic parameters and the geometric parameters of the turbine.

$$a_{u,d} = \begin{cases} \tilde{F}_{x\,u,d} + a_{u,d}^2 & 0.0 \le a_{u,d} \le 1/3 \\ \tilde{F}_{x\,u,d} + \frac{1}{4}(5 - 3a_{u,d})a_{u,d} & 1/3 < a_{u,d} \le 1.0 \end{cases} \tag{6}$$

$$\tilde{F}_{xu} = \frac{B\,C}{8\pi R\,|sin(\theta)|}\left(\frac{W_u}{U_\infty}\right)^2 (C_n sin\theta - C_t cos\theta) \tag{7}$$

$$\tilde{F}_{x\,d} = \frac{B\,C}{8\pi\rho R\,|sin(\theta)|}\left(\frac{W_d}{U_\infty(1 - 2a_u)}\right)^2 (C_n sin\theta - C_t cos\theta) \tag{8}$$

The resolution of the equations obtained is done by the iterative numerical method and results in obtaining adimensional coefficient C_t of the tangential force T and the relative speed $W_{u,d}$. Therefore, we can calculate the torque for a blade with respect to the axis of rotation according to the following formula:

$$T_i(\theta) = \frac{1}{2}\rho W_{u,d}^2 (HC) C_t R \tag{9}$$

For a tidal turbine with B blades, the instantaneous global torque provided by the blades will be determined by equation (10) [4] and [18].

$$T(\theta) = \sum_{i=1}^{B} T_i(\theta_i)\,,avec\ \theta_{i+1} = \theta_i + \frac{360}{B} \tag{10}$$

The average torques for the upstream and downstream half-discs of the turbine are respectively evaluated by the following equation (11) and equation (12) **[19]:**

$$T_{avg,u} = B\sum_{i=1}^{N_\theta} \frac{\left(\frac{1}{2}\rho W_u^2 (HC) C_t R\right)}{N_\theta} \tag{11}$$

$$T_{avg,d} = B\sum_{i=1}^{N_\theta} \frac{\left(\frac{1}{2}\rho W_d^2 (HC) C_t R\right)}{N_\theta} \tag{12}$$

The average total torque of the tidal turbine over one revolution can be expressed by equation (13).

$$T_{avg} = \frac{1}{2}(T_{avg,u} + T_{avg,d}) \tag{13}$$

The torque and power coefficients are calculated respectively by the following equations (14) and (15) **[19] and [23]:**

$$C_{T_{avg}} = \frac{T_{avg}}{\frac{1}{2}\rho U_\infty^2 (2RH) R} \tag{14}$$

$$C_P = \lambda C_{T_{avg}} \tag{15}$$

2.2.4. Determination of the torque and power of a column of vertical axis tidal turbines using the DMST model

For a column made up of three identical turbines, the torque supplied is expressed by [4]:

$$T_{tour}(\theta) = T_{turbine1}(\theta) + T_{turbine2}(\theta) + T_{turbine3}(\theta) \tag{16}$$

Furthermore, for a column made up of three turbines, we will have a total power [4]:

$$P_{tour}(\theta) = P_{turbine1}(\theta) + P_{turbine2}(\theta) + P_{turbine3}(\theta) \tag{17}$$

2.3. PMSG dynamic model in the dq axis

2.3.1. Modeling of the synchronous machine in the two-phase reference frame (dq)

The considered permanent magnet synchronous machine is a radial type magnetization machine with surface mounted magnets.

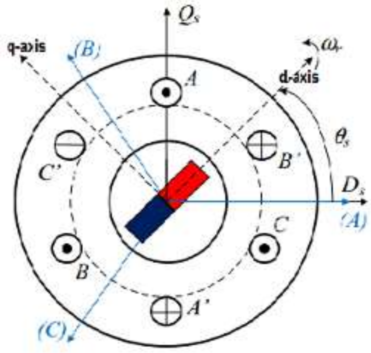

Figure 6: PMSG cross section, Reference frame (a, b, c) and Reference frame (d, q) [12]

Using the generating convention, the equations for the machine voltage in the Park frame are as follows:

$$\begin{cases} V_d = -R_s \mathrm{i_d} - \mathrm{L_d}\dfrac{d\mathrm{i_d}}{dt} + p\omega \mathrm{L_q i_q} \\ V_q = -R_s \mathrm{i_q} - \mathrm{L_q}\dfrac{d\mathrm{i_q}}{dt} - p\omega \mathrm{L_d i_d} + p\omega \psi_\mathrm{f} \end{cases} \tag{18}$$

The expression of the electromagnetic torque for the cylindrical rotor will be expressed as follows:

$$\boldsymbol{T_{em} = \frac{3}{2} p \psi_f I_{qs}} \tag{19}$$

The differential equation which characterizes the mechanical behavior of the turbine and generator assembly is given by:

$$\mathrm{T}_{tur} - \mathrm{T}_{em} = \mathrm{J}_{tot}\frac{d\Omega_{tur}}{dt} + \mathrm{f}_v \Omega_{tur} \tag{20}$$

Which, J_{tot} is the total inertia of the turbine and the generator [kg.m^2]; T_{tur} presents the torque of the turbine [Nm], T_{em} is the electromagnetic torque of the generator [Nm]; f_v represents the coefficient of viscous friction [kg/s] and Ω_{tur} is the speed of rotation of the turbine or generator [tr/s].

2.3.2. *Global model of the PMSG under RL load*

The overall model of the *PMSG* under load with Z line = 0 is presented in Figure 7.

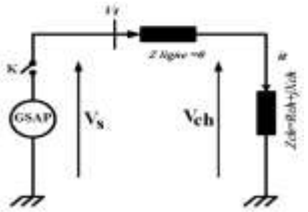

Figure 7: Permanent magnet synchronous generator connected to a load

The R-L load model in the Park frame is [26]:

$$\begin{cases} V_d = R_{ch}\mathrm{i_d} + \mathrm{L_{ch}}\dfrac{d\mathrm{i_d}}{dt} - p\omega \mathrm{L_{ch} i_q} \\ V_q = R_{ch}\mathrm{i_q} + \mathrm{L_{ch}}\dfrac{d\mathrm{i_q}}{dt} + p\omega \mathrm{L_{ch} i_d} \end{cases} \tag{21}$$

2.4. Mitigation by controlling the tidal turbine of the Turbine torque impact

2.4.1. Optimal TSR MPPT Control System

Insertion of a control system in the tidal turbine, according to figure 8, makes it possible to improve the output voltage of the generator.

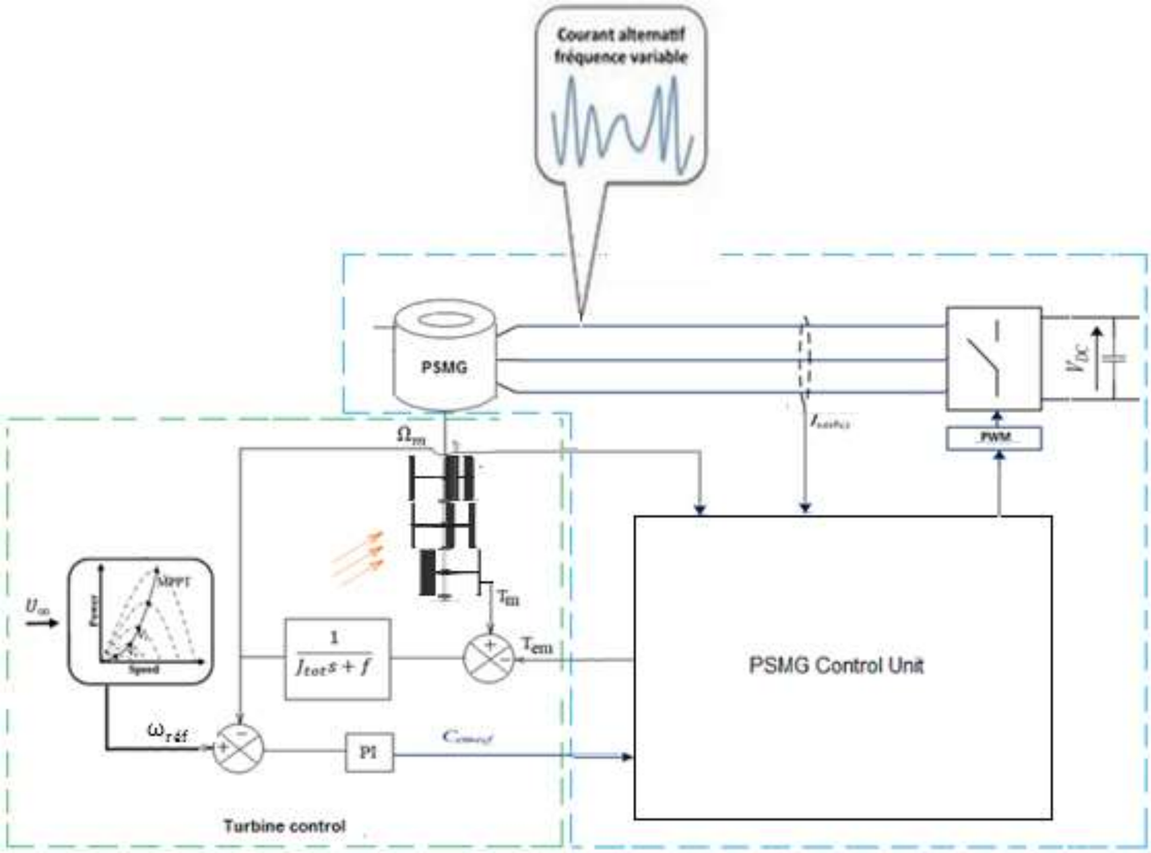

Figure 8: Control of the tidal turbine

The control system is composed of the optimal TSR MPPT control to extract maximum power from the water flow, the PWM command for the rectifier, and the PI correctors for the PMSG regulations.

2.4.2. Turbines column data

Column of three turbines were considered, according to Figure 9, with 1.5 [m/s] of flow speed, and all offset by 40°. The main characteristics of each turbine are summarized in Table 1.

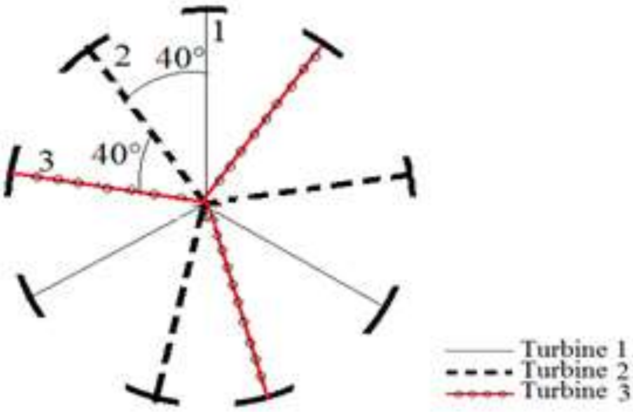

Figure 9: Top view of column of three turbines offset by 40°

III. RESULTS

3.1. Torque and power evolutions

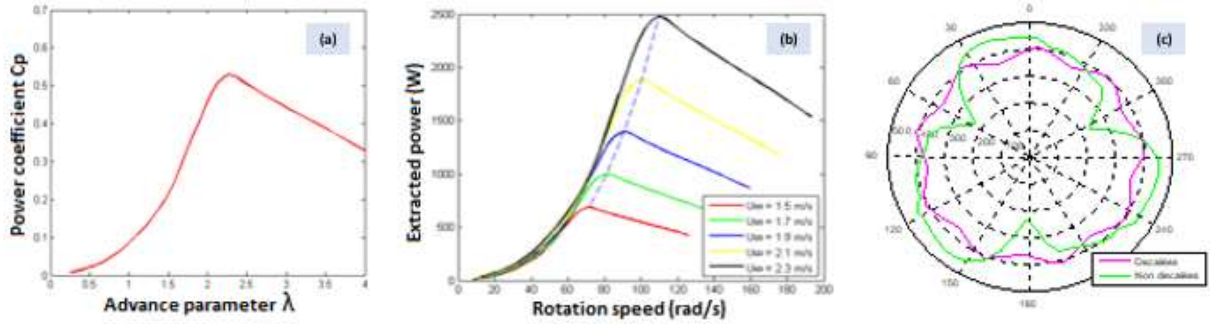

Figure 10: Evolution of (a) the power coefficient as a function of the advance parameter, (b) Power extracted as a function of flow and rotation speeds, and (c) Torque rosette of the column of three turbines

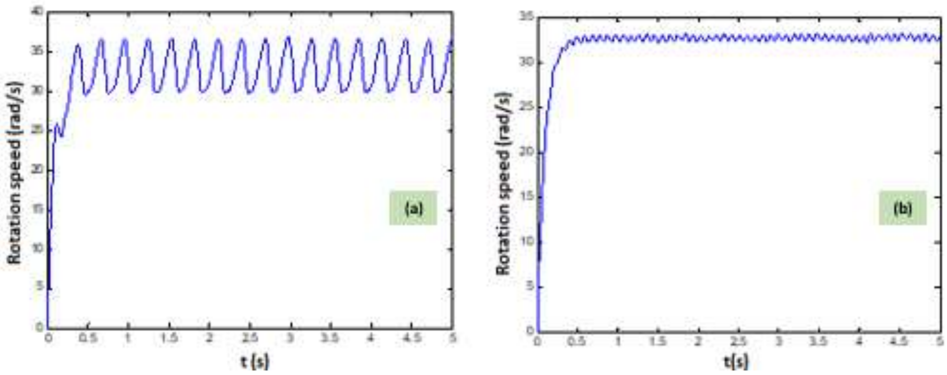

Figure 11: Rotation speeds in the absence of a control system, (a) With column of three non-offset turbines, and (b) With column of three offset turbines

3.2. Changes in rotation speeds in the presence of a control system

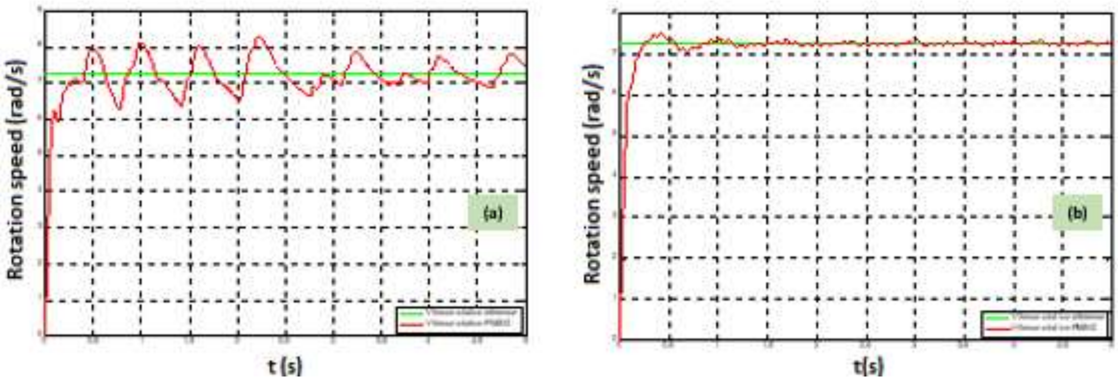

Figure 12: Rotation speeds in the presence of a control system, (a) With column of three non-offset turbines, and (b) With column of three offset turbines

3.3. Changes in currents and voltages in the absence of a control system

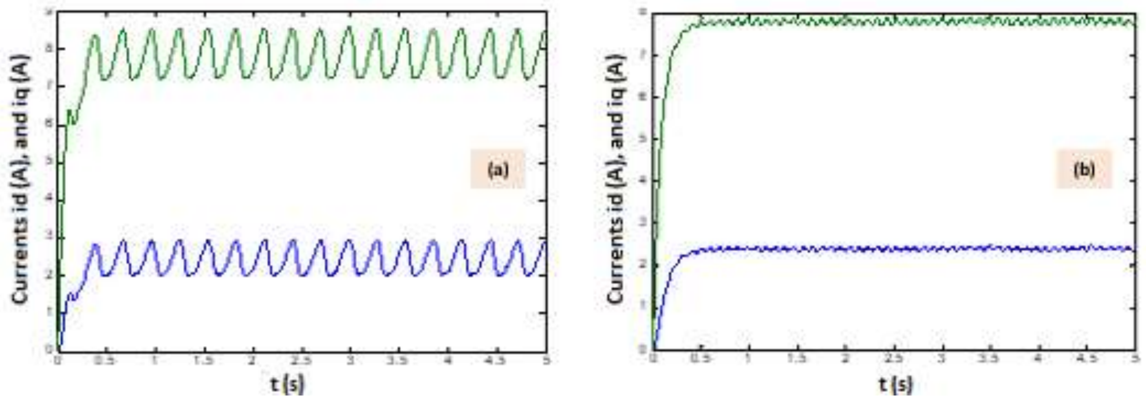

Figure 13: Currents id and iq in the absence of a control system, (a) With column of three non-offset turbines, and (b) With column of three offset turbines

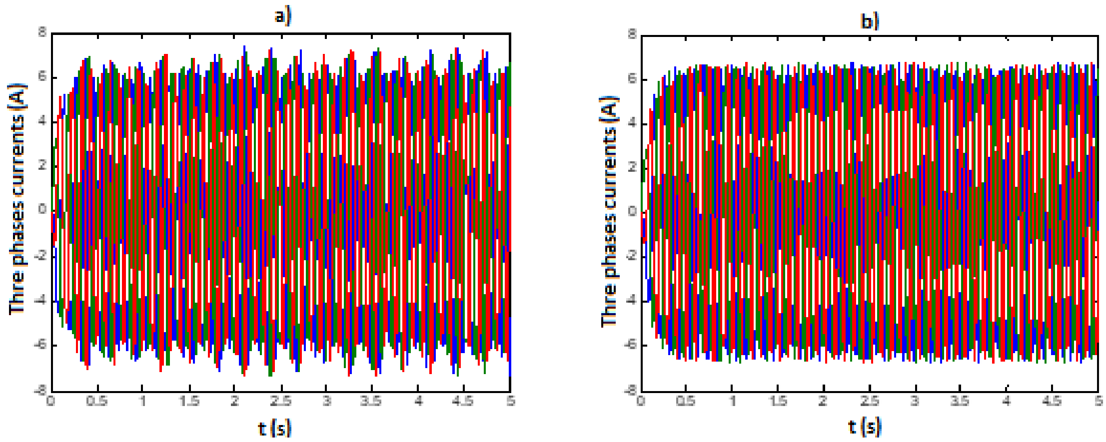

Figure 14: Currents Ia, Ib, and Ic in the absence of a control system, a) With column of three non-offset turbines, and b) With column of three offset turbines

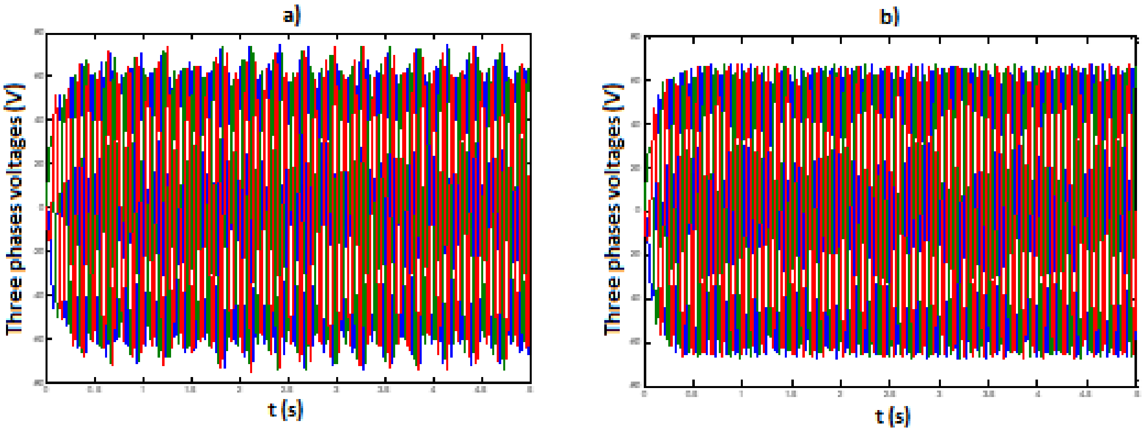

Figure 15: Voltages Va, Vb, and Vc in the absence of a control system, a) With column of three non-offset turbines, and b) With column of three offset turbines

3.4. Evolutions of currents and voltages in the presence of a control system

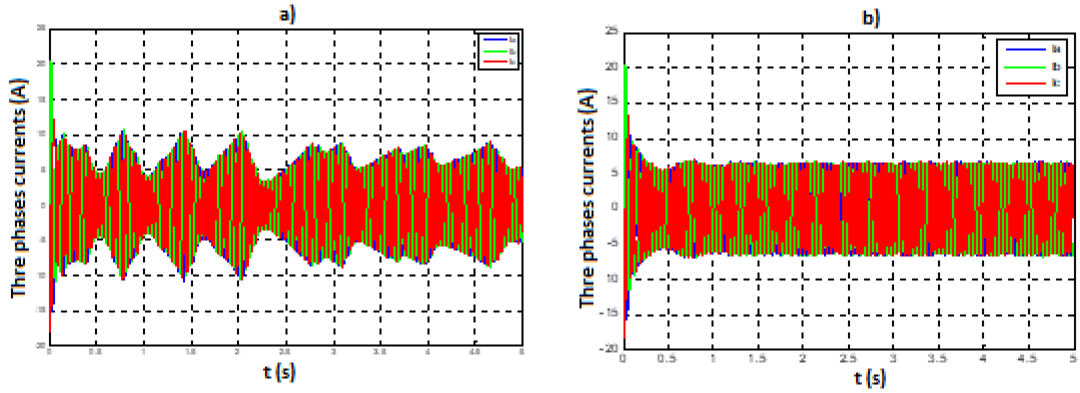

Figure 16: Currents Ia, Ib, and Ic in the presence of a control system, a) With column of three non-offset turbines and b) With column of three offset turbines

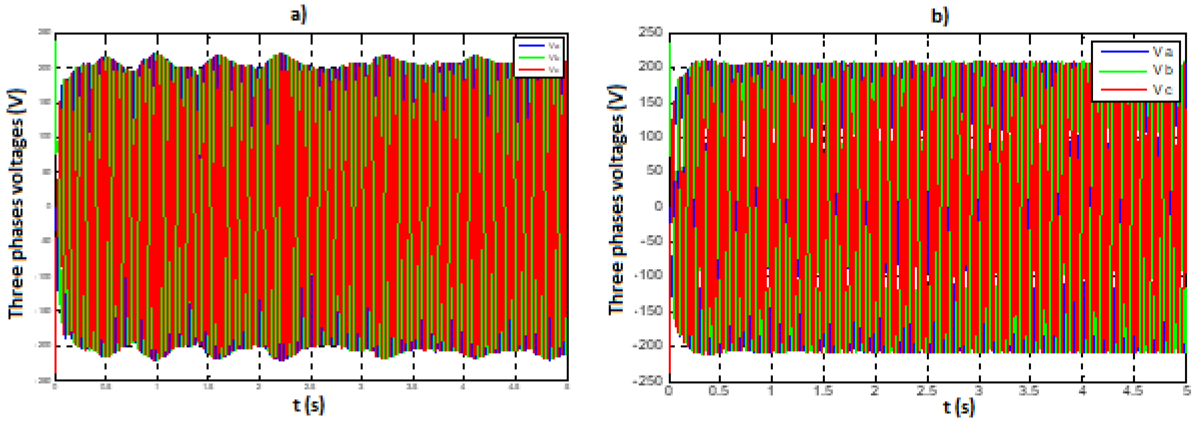

Figure 17: Voltages Va, Vb, and Vc in the presence of a control system, a) With column of three non-offset turbines and b) With column of three offset turbines

IV. Discussions

The numerical simulation of the column of three tidal turbines based on the DMST method and with the flow $U_{\infty} de\ 1.5\ m/s$ was carried out. Figure *10-a* shows an evolution of power coefficient C_P from 0 to 55.07% being lower than the Betz limit (59.25%). The top of this curve corresponds to the maximum power coefficient (or maximum efficiency) $C_{pmax} de\ 0.55$ and the optimal advance parameter $\lambda_{opt}\ de\ 2.2$. It constitutes the optimal operating point of the turbine. This result confirms the work carried out by Bossard [23] which shows that the optimal specific speed of tidal turbines is of the order of 2. We note that this power coefficient curve (*figure 10-a*) has the same appearance predicted in the *section 2.2.1* (*Figure 2*). According to *Figure 10*– b, we see the different levels of average power as a function of rotation speed which increase following the increase U_{∞}. This characteristic is exploited in the MPPT (Maximum Power Point Tracking) control strategy of the tidal turbine, making it possible to extract the maximum power for a given flow speed.

At the flow of $U_{\infty} = 1.5\ m/s$ and at the optimal operating point, (λ_{opt} , C_{pmax})that is to say the power supplied by the column of three turbines is maximum 2062 W corresponding to the optimal average rotation speed of 7.25 rad/s, *Figure 10-c* shows the evolution of the torques as a function of the azimuthal position of the blades. The column torque rosette of three offset turbines oscillates between 361.88 Nm and 408.79 Nm while the other with three non-offset turbines varies between 233.27 Nm and 457.02 Nm. When the three turbines are offset, we observe the images of the 9 blades on the torque rosette (*Figure 10-c*). The presence of two driving zones and two braking zones, according to the operating principle detailed in *section 2.2.2* (*Figure 4*), is noted in the evolution of the torques. The torque with offset turbines is smoother than that with non-offset turbines (*Figure 10-c*).

Therefore, the rotation speeds with non-offset turbines oscillate at higher amplitudes than with offset turbines according to *Figure 11 and Figure 12.* Same impacts were observed on the currents in the Park frame (d, q) of *Figure 13* and on the envelopes of those in the real marks (a, b, c) of *Figure 14 and Figure 16.* The currents are, in accordance with the results encountered in the literature, the images of the couples.

The envelopes of the voltage amplitudes shown in *Figure 17-ab* in the real benchmarks (a, b, c) for the tidal turbine equipped with a control system are smoother compared to those of Figure *15-ab* relating to the tidal turbine without control system. Furthermore, the error between the reference speed and the rotational speed of the PMSG in the case of offset turbines is smaller (*Figure 12-b*) compared to that in the case of non-offset turbines (*Figure 12-a*). Then, the voltages output from the PMSG in the case of offset turbines *Figure 17-b* have the best appearances than those in the case of non-offset turbines.

Due to the fact that the reference speed considered in the control of the turbines column is a constant according to formula (3), these results, on the regulation effect for the voltages output from PMSG, can be improved by looking for the speed of reference rotation as instantaneous in order to minimize the error between the measured rotation speed and the reference speed. In fact, the turbine actually rotates with oscillating speed because it provides a fluctuating torque.

V. Conclusion

We determined by the multiple current tube model with double actuator disks, the power coefficient and the mechanical torque of a column of vertical axis tidal turbines, each turbine of which has a radius of 455mm and a height of 824mm. For a flow of 1.5 m/s corresponding to the maximum average power coefficient, the column of three offset turbines provides a smoother torque oscillating between 361.88 Nm and 408.79 Nm whereas with three non-offset turbines, it is much fluctuated and varies between 233.27 Nm and 457.02 Nm. With these torques, the simulation of the column assembly of three turbines and PMSG made it possible to observe that the rotation speeds, currents and tensions of the PMSG with non-offset turbines oscillate at higher amplitudes than with offset turbines. The voltage amplitude envelopes for the tidal turbine equipped with a control system are smoother compared to those of the tidal turbine without a control system. In addition, with the control system, the voltages output from the PMSG in the case of offset turbines have the best appearances than those in the case of non-shifted turbines as the error between the reference speed and the rotation speed of the PMSG in the case of offset turbines is lower compared to that in the case of non-offset turbines. In order to minimize the error between the measured rotation speed and the reference one, the search for the more precise reference rotation speed is necessary.

Appendix

Setting	Symbol	Quantity	Unit
Rope length	VS	156	[mm]
Turbine radius	R	455	[mm]
Impeller height	H	824	[mm]
Pitch angle	β	0	[°]

Table 1: Dimensions of the tidal turbines column

VI. REFERENCES

1. H. Baccar and al, "Maximisation du Rendement d'Un Générateur Eolien à Base d'Une Génératrice Synchrone à Aimant Permanent", https://www.researchgate.net/publication/320347285, 2017.
2. T. Randriamaitso, R. Manasina, F. P. Andriniriniaimalaza and J. M. Razafimahenina “Study of the torque impact on the Permanent Magnet Synchronous Generator voltages output for a vertical axis tidal turbine”,

Article, International Journal of Innovative Science, Engineering & Technology (IJISET), Vol. 8 Issue 7, July 2021, ISSN (Online) 2348 – 7968 | Impact Factor (2020) – 6.72, www.ijiset.com.
3. M. Dansoko, "Modélisation et commande non linéaire des hydroliennes couplées à un réseau électrique", Thèse de Doctorat, Université Paris 13-Sorbonne Paris-Cité, 2014.
4. A. M. Andreica, "Optimisation énergétique de chaînes de conversion hydroliennes – modélisation, commandes et réalisations expérimentales", Thèse de Doctorat, Institut Polytechnique de Grenoble, 2009.
5. A. Seck, "Optimisation et commande d'une génératrice pentaphasée pour applications hydroliennes", Thèse de doctorat, Université de Nantes, 2019.
6. M. Andreica, S. Bacha, D. Roye and J. Guiraud, "Intégration d'une hydrolienne au réseau, MPPT et qualité de l'énergie", Article, Revue des Énergies Renouvelables Vol. 11 N°4 (2008) 493 – 502.
7. P. Delafin, "Analyse de l'écoulement transitionnel sur un hydrofoil. Application aux hydroliennes à axe transverse avec contrôle actif de l'angle de calage", Thèse de doctorat, Université de Bretagne Occidentale, 2014.
8. T. Jaquier, "Hydroliennes à flux transverse: Développement d'un prototype HARVEST en canal", Thèse de doctorat, Université de Grenoble, 2011.
9. L. Guangnian, C. Qingren and G. Hanbin, "An Unsteady Boundary Element Model for Hydrodynamic Performance of a Multi-Blade Vertical-Axis Tidal Turbine", Article, www.mdpi.com/journal/water, Water 2018, 10, 1413.
10. M. Wen, Y. Ren and N. Srikanth, "Review of Maximum Power Point Tracking Algorithm for Tidal Turbine Generator", Proceedings of 3rd Asian Wave and Tidal Energy Conference 2016 (AWTEC 2016).
11. W. Jaikhang, S. Tunyasrirut, "Artificial Intelligent Tuning PI Controller on Wind Turbine System with Three-Phase Grid Connected System", Article, Indonesian Journal of Electrical Engineering and Informatics (IJEEI). Vol. 7, No. 4, pp. 703~720, ISSN: 2089-3272, DOI: 10.11591/ijeei.v7i4.1329, 2019.
12. M. Aimene, "Services au système et gestion d'interactions énergétiques transitoires dans un parc éolien offshore", Thèse de doctorat, Normandie Université, 2016.
13. S. Apelfröjd, R. Ekström, K. Thomas and M. Leijon, "A Back-to-Back 2L-3L Grid Integration of a Marine Current Energy Converter", Article, Energies 2015, 8, 808-820; doi:10.3390/en 8020808, ISSN 1996-1073, www.mdpi.com/journal/energies.
14. S. Toumi, Y. Amirat, E. Elbouchikhi , M. Trabelsi, M. Benbouzid, M. Faouzi Mimouni, "A comparison of fault-tolerant control strategies for a PMSG-based marine current turbine system under generatorside converter faulty conditions", Article, Journal of Electrical Systems (JES), 13-3 (2017): 472-488.
15. D. Ikni, M. S. Camara, M. B. Camara, B. Dakyo, H. Gualous. "Permanent Magnet Synchronous Generators for Large Offshore Wind Farm Connected to Grid - Comparative Study between DC and AC Configurations", Article, INTERNATIONAL JOURNAL OF RENEWABLE ENERGY RESEARCH, Djamel Ikni et al., Vol.4, No.2, 2014.
16. N. Batista1, R. Melicio and V. Mendes, "Darrieus-type vertical axis rotary-wings with a new design approach grounded in double-multiple streamtube performance prediction model", Article, AIMS Energy, 6(5): 673–694, http://www.aimspress.com/journal/energy, 2018.
17. H. E. Saber, E. M. Attia and H. A. El Gamal, "Analysis of Straight Bladed Vertical Axis Wind Turbine", Article, International Journal of Engineering Research & Technology (IJERT), ISSN: 2278-0181, Vol. 4 Issue 07, July-2015.
18. R. Manasina, "Modélisation numérique et optimisation des hydroliennes à axe vertical avec des méthodes évolutionnaires", Thèse de doctorat, École doctorale physique et applications, Université d'Antananarivo Madagascar, 2016.
19. A. M. Biadgo, A. Simonovic, D. Komarov and S. Stupar, "Numerical and Analytical Investigation of Vertical Axis Wind Turbine", Article, Faculty of Mechanical Engineering, Belgrade, FME Transactions (2013) 41, 49-58.
20. H. Q. Minh, N. Frédéric, N. Essounbouli, A. Hamzaoui, "Control of permanent magnet synchronous generator wind turbine for standalone system using fuzzy logic", Article, https://www.researchgate.net/publication/264922117, EUSFLAT-LFA 2011.

21. Z. Zhou, F. Scuiller, J. F. Charpentier, M. Benbouzid, T. Tang, "Power Smoothing Control in a Grid-Connected Marine Current Turbine System for Compensating Swell Effect", Article, IEEE TRANSACTIONS ON SUSTAINABLE ENERGY, 2013, 4 (3), pp.816-826.
22. S. Mitchell1, I. Ogbonna1, and K. Volkov, "Improvement of Self-Starting Capabilities of Vertical Axis Wind Turbines with New Design of Turbine Blades", Article, Sustainability 2021, 13, 3854, https://www.mdpi.com/journal/sustainability.
23. G. Abdalrahman, W. Meleka , F. Lienb, "Pitch angle control for a small-scale Darrieus vertical axis wind turbine with straight blades (H-Type VAWT) ", Article, Renewable Energy 114 (2017) 1353 – 1362.
24. J. Bossard, "Caractérisation expérimentale du décrochage dynamique dans les hydroliennes à flux transverse par la méthode PIV (Particle Image Velocimetry). Comparaison avec les résultats issus des simulations numériques", Thèse de doctorat, Université de Grenoble, 2012.